Jordanian Journal of Computers and Information Technology (JJCIT), Vol. 10, No. 04, December 2024.

LOW-PROFILE BI-SLOT DUAL-BAND (2.45/5.76GHZ) ANTENNA FOR WIRELESS COMMUNICATION SYSTEMS

Ahmad Abbas AL Rimi[1*], Asmaa Zugari[1], Mohssine El Ouahabi[2] and Mohsine Khalladi[1]

(Received: 7-May-2024, Revised: 4-Jul.-2024, Accepted: 27-Jul.-2024)

ABSTRACT

This article presents a compact dual-band patch antenna designed for wireless communication systems. The proposed antenna design operates efficiently at both 2.45 GHz and 5.76 GHz achieving high performance despite its compact size. The Defected Microstrip Structure (DMS) is used to create the desired frequency bands and improve the impedance matching at the respective required frequencies, respectively. The antenna is manufactured on a low-cost FR-4 substrate, with dimensions of 27 mm × 27 mm × 1.6 mm. The simulated radiation efficiencies at 2.45 GHz and5.76 GHz are 95% and 73%, respectively. In addition, the gain of the suggested antenna is more than 2.65 dB and around 2.84 dB at the desired frequency bands. The suggested antenna is simulated, manufactured, tested and verified practically. The return losses measured in the lower and upper resonance bands are 29.94% (covering the frequency range from 2.13 to 2.88 GHz) and 6.2% (covering the frequency range from 5.65 to 6.01 GHz), respectively. The radiation pattern is measured and compared with the simulation one. The design is simple, easy to carry on and is very compact, while enabling seamless operation across two different frequency bands, which makes it suitable for diverse wireless applications.

KEYWORDS

Compact, Dual-band, DMS, WLAN.

1. INTRODUCTION

Wireless communication has undergone rapid advances in contemporary society, encompassing a variety of technical fields. Following the FCC's announcement allowing individuals to use medical, industrial and scientific frequencies without the need for a licence, the scientific community has been provided with an important opportunity to create wireless devices suitable for short-range communication. The most notable examples are Bluetooth, which operates in the globally allocated 2.4 GHz ISM band [1] and wireless local area networks (WLANs), which operate at frequencies of 5.2 GHz and 5.8 GHz. WLANs were conceived as adaptable data-communication systems, serving as substitutes for or extensions to wired local networks. Using radio-frequency technology, these networks send and receive data wirelessly in the atmosphere, significantly reducing reliance on wired connections and seamlessly integrating uninterrupted connectivity with user mobility. In today's landscape, wireless LANs are rapidly gaining popularity in diverse sectors, such as healthcare, manufacturing and academia. These industries have reaped substantial benefits from portable devices that enable real-time transfer of data to central processing centres. In addition, wireless local area networks are increasingly recognized as a reliable and cost-effective means of achieving fast wireless internet access. They are being adopted as versatile connectivity solutions in a wide range of applications [2].

The IEEE 802.11 WLAN standards encompass three operational frequency bands: 2.4 GHz (2.400 GHz - 2.484 GHz), 5.2 GHz (5.150 GHz - 5.350 GHz) and 5.8 GHz (5.725 GHz - 5.825 GHz). In the IEEE 802.11a standard, WLANs operate within the higher-frequency range, covering the range of 5.15 GHz to 5.35 GHz and 5.725 GHz to 5.825 GHz. On the other hand, WLANs that adhere to the IEEE 802.11b/g standards use the 2.4 GHz band, which extends from 2.4 GHz to 2.484 GHz [2][3][4]. In the contemporary landscape, dual-band WLAN systems, which include IEEE 802.11a /b /g standards are becoming increasingly popular [5]. Consequently, to meet the demands of wireless communication, it is necessary to develop compact, high-performance antennas capable of operating in the dual bands of 2.4 and 5.8 GHz, while at the same time offering exceptional radiation properties

1. A. AL Rimi (Corresponding Author), A. Zugari and M. Khalladi are with Information Systems and Telecommunications Laboratory, University of Abdelmalek Essaadi, Faculty of Science Tetuan, Morocco. Emails: alrimiahmed75@gmail.com, asmaa.zugari@gmail.com and m_khall@hotmail.com
2. M. El Ouahabi is with National School of Applied Sciences, University of Abdelmalek Essaadi, Email: moelouahabi@uae.ac.ma

[2], [6]. Nonetheless, the design of compact dual-band antennas is a major challenge, given the need to meet wide-bandwidth requirements, as well as to achieve a balanced radiation pattern, constant gain, compact size and simple manufacturing processes [7][8][9]. On the other hand, the narrow-band antenna can be transformed into a multiband antenna by introducing a slit or slot at strategically chosen positions on its patch or ground plane. The dimensions, geometry and position of this slot are crucial to the creation of resonances and band characteristics [10]. A number of dual-band microstrip antennas have been reported in the literature, but they typically exhibit rather large sizes and relatively complex designs. For instance, a dual-band printed slot antenna using the Cantor fractal has achieved two operating frequency bands of 2.35–3.61 GHz and 5.15–6.25 GHz; achieving this performance necessitated large physical dimensions of 50 x 50 mm² [11]. Similarly, an annular Koch snowflake fractal antenna designed for dual-band performance covered 2.24–2.93 GHz and 4.48–5.54 GHz, with dimensions of 40 × 40 mm² [12]. A dual Wide Band Monopole Antenna for WiFi and WiMAX systems, has been designed to cover 2.3–2.98 GHz and 5.13–7.75 GHz, with dimensions of 40 × 44 mm² [13]. A dual Wideband Monopole antenna for GSM/UMTS/LTE/WiFi/and Lower UWB applications consists of two sickle-shaped radiators and a slotted ground plane, achieving operating bands of 1.5–2.8 GHz and 3.2–6 GHz, but it possesses a large size of 57 × 37.5 mm² and a relatively complex design [14]. A DGS antenna designed for medical applications has been published. It operates at two frequency bands with dimensions of 58 x 40 mm² [15]. A dual-band microstrip antenna using a polarization conversion metasurface structure is proposed in [16], with dimensions of 40 × 49 mm². A dual-band semi-circular patch antenna for WiMAX and WiFi-5/6 applications witch covers 2.39–3.75 GHz and 5.39–7.18 GHz, with dimensions of 30 × 40 mm² was proposed in [17]. In [18], a dual-band antenna for WiMax and Wi-Fi applications is introduced with dimensions of 40 × 40 mm². Reference [19] incorporates a Dual-Band Microstrip Patch Antenna Design Using C-shaped slot to cover the 2.4 and 5 GHz frequency bands, with dimensions of 53 × 49 mm².

This paper proposes a compact dual-band patch antenna that operates efficiently at 2.45 GHz and 5.76 GHz, achieving high efficiencies of over 95% and 73% in both operating bands. The antenna attains gains of 2.65 dB and 2.84 dB, respectively. The Defected Microstrip Structure (DMS) technique is used to achieve the desired frequency bands and enhance impedance matching at both frequencies.

The proposed antenna has been simulated, manufactured, tested and practically verified, with results showing good agreement with simulations. These results demonstrate the antenna's suitability for WLAN, ISM and WiMAX applications. Additionally, it is characterized by its small size, ease of manufacture and smooth operation across two different frequency bands.

The design structure, simulated and measured results, analysis and concluding remarks are presented in Sections 2, 3, 4, 5 and 6.

2. ANTENNA DESIGN EVOLUTION

2.1 Design Process

The antenna design process is structured into four stages. Figure 1 depicts the evolution of the proposed antenna, while Figure 2 presents the simulated reflection-coefficient curves corresponding to each stage.

In Step 1, the design of the initial rectangular patch antenna is calculated using the well-known transmission line theory [20]:

$$LP = \frac{C}{2 f_r \sqrt{\varepsilon reff}} - 0.824h - \left(\frac{(\varepsilon reff + 0.3)(\frac{W p}{h} + 0.264)}{(\varepsilon reff + 0.258)(\frac{W p}{h} + 0.8)} \right)$$

$$W p = \frac{C}{2 f_r \sqrt{\frac{\varepsilon r + 1}{2}}}$$

$$\varepsilon_{reff} = \frac{\varepsilon_r + 1}{2} + \frac{\varepsilon_r - 1}{2} \left(1 + 12 \frac{h}{W} \right)^{-0.5}$$

Jordanian Journal of Computers and Information Technology (JJCIT), Vol. 10, No. 04, December 2024.

where, Lp is the length of the patcn, Wp is the width of the patcn, C is the speed of light (3×10^8 m/s), fr is the resonant frequency, ϵr is the substrate relative permittivity and h is the substrate thickness.

In the second stage, enhancing impedance matching with a reduced ground plane leads to a resonant frequency of 5.59 GHz. The third stage introduces a rectangular slot (L2 x W1) on the top of the patch, resulting in a resonant frequency of 2.78 GHz. Finally, in the fourth stage, adding another rectangular open-ended slot (L2 x W1) below the patch produces two resonant frequencies at 2.9 GHz and 6.27 GHz.

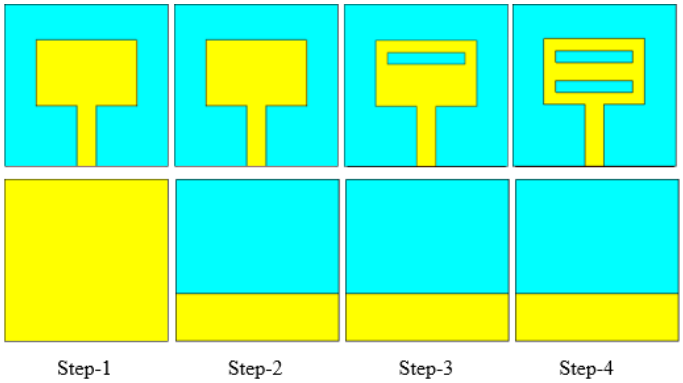

Figure 1. Design procedure of the proposed antenna.

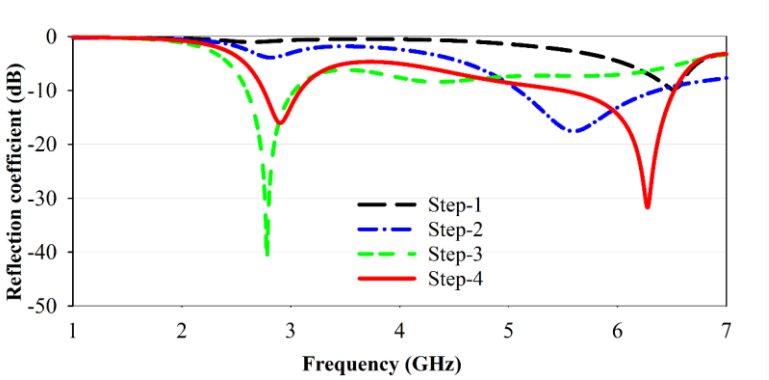

Figure 2. Simulated reflection coefficients for all design steps.

2.2 Final Structure and Dimensions

The design of the proposed antenna and its corresponding prototype are illustrated in Figure 3. The antenna is manufactured on an FR-4 substrate, which has a relative permittivity of 4.3, a height (h) of 1.6 mm and a loss tangent of 0.025. A 50-ohm microstrip line is used to connect the antenna to an external source *via* an SMA connector. Dual-band radiation at the specified frequencies is achieved by drilling two parallel rectangular slots in the patch and utilizing defected ground structure (DMS) technology to improve impedance matching. Both the patch and ground plane are made of copper. The optimal dimensions of the antenna, determined through a parametric study using CST Microwave Studio, are outlined in Table 1. Computer Simulation Technology (CST) is used to design and simulate the proposed antenna.

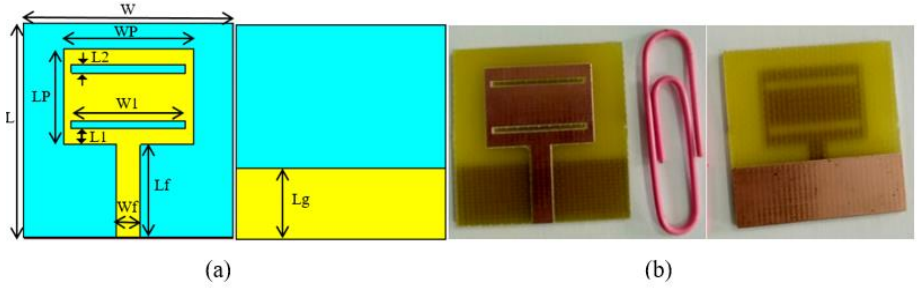

Figure 3. (a) Top and bottom views of the designed antenna geometry, (b) The manufactured prototype.

Table 1. Optimized dimensions of the proposed antenna.

Parameters	L	W	LP	WP	Lf	Wf	Lg	L1	L2	W1	h
Value(mm)	27	27	12	16.7	11.7	3.137	9	2	1	14.7	1.6

3. PARAMETRIC STUDIES

The main purpose of this section is to study the effect of antenna parameters on resonant frequencies and matching. This analysis aims to determine the optimal values for the two rectangular slots etched inside the patch using the DMS technique. This is achieved by adjusting a single parameter while maintaining others constant.

3.1 Effect of L1 and L2

As shown in Figure 4(a), modifications in the position of the two rectangular slots from L1 = 1 mm to L1 = 3 mm leads to a decrease in return loss at the lower frequency of 2.45 GHz, while at both L1 = 1 mm and L1 = 3 mm, the upper frequency of 5.76 GHz is entirely absent. Moreover, as depicted in Figure 4(b), altering the width of the rectangular slot from L2= 0.5 mm to L2= 1.5 mm results in a decrease in return loss at the higher frequency. Additionally, this modification causes a shift in the upper frequency from 5.82 GHz to 5.66 GHz up to 5.76 GHz, while the lower frequency of 2.45 GHz remains unaffected. It is observed that the optimal outcome is achieved for L1= 2 mm and L2= 1 mm in both frequency bands.

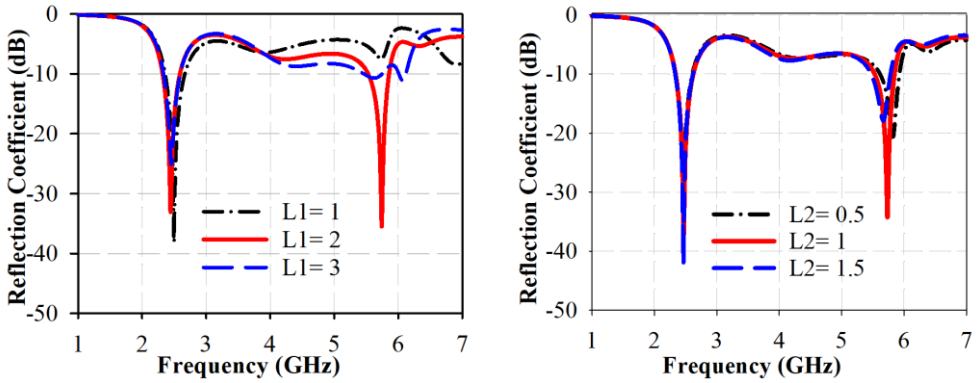

(a) (b)

Figure 4. Simulated S_{11} parameter for various values of (a) L1 and (b) L2.

3.2 Effect of W1 and Lg

Figure 5(a) shows the simulated reflection coefficient of W1; when W1 is increased from 13.7 mm to 15.7 mm, the upper resonant frequency decreases progressively from 6.15 GHz to 5.76 GHz and finally to 5.4 GHz. Our objective is to achieve a resonant frequency of 5.76 GHz, the optimal value is observed at W1 = 14.7 mm. Also, as observed in Figure 5(b), the simulated reflection coefficient decreases when the Lg value increases or decreases from 9 mm, indicating that 9 mm is the optimal value.

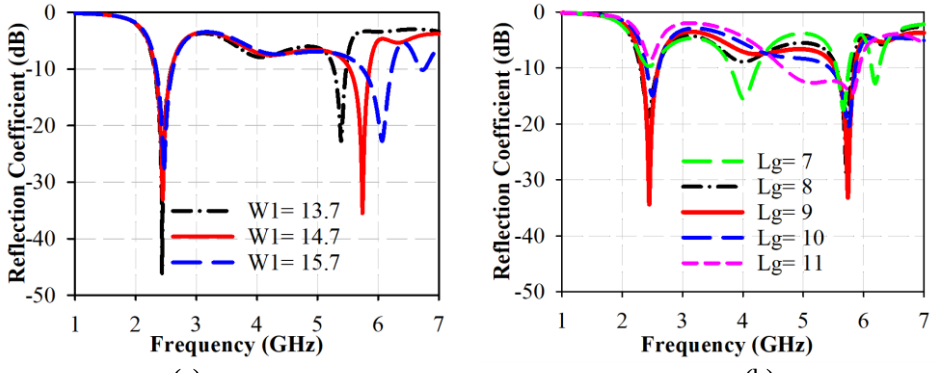

(a) (b)

Figure 5. Simulated S_{11} parameter for different values of (a) W1 and (b) Lg.

Jordanian Journal of Computers and Information Technology (JJCIT), Vol. 10, No. 04, December 2024.

4. SIMULATION RESULTS AND DISCUSSION

The designed antenna is manufactured using the LPKF ProtoMat E33 milling machine. The Rohde and Schwarz ZVB 20 Vector Network Analyzer is utilized to measure the S-parameters, as depicted in Figure 6(b). It is evident that there is acceptable agreement between the measurements and the simulation results as can be seen in Figure 6(a). The impedance bandwidths (S_{11} < -10 dB) of the suggested antenna are (2.13–2.88 GHz), corresponding to a range of 29.94% (lower-frequency band) and (5.65–6.01 GHz), corresponding to a range of 6.2% (higher-frequency band), respectively. Figure 7(a) shows the VSWR graph at the center frequencies for the proposed antenna, with values less than 2. Specifically, the designed antenna has a VSWR of 1.06 at 2.45 GHz and 1.11 at 5.76 GHz, indicating favorable impedance matching. Figure 7(b) presents the Z-parameter of the antenna, demonstrating that the impedance is approximately 50 Ohms at both 2.45 GHz and 5.76 GHz, confirming that the antenna provides perfect impedance matching.

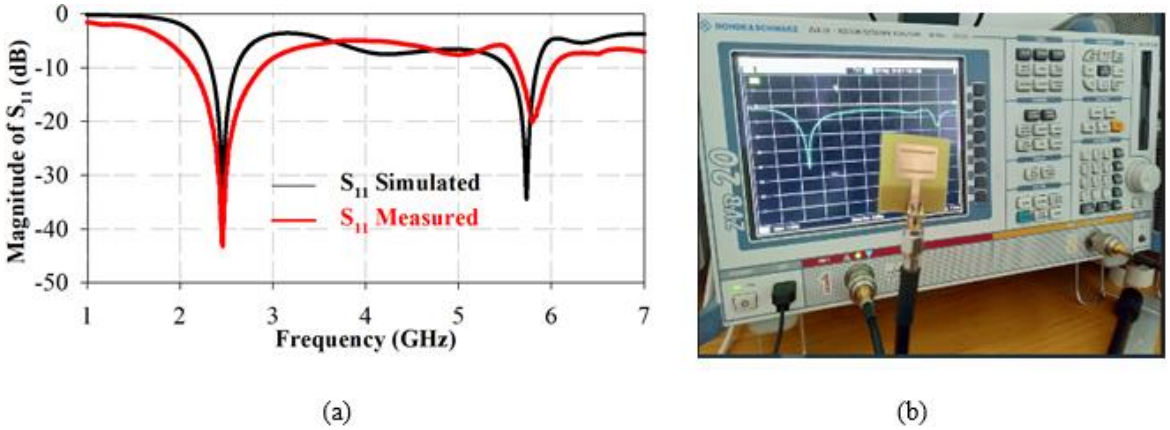

Figure 6. (a) Measured and simulated magnitude of S_{11}, (b) Measurement setup.

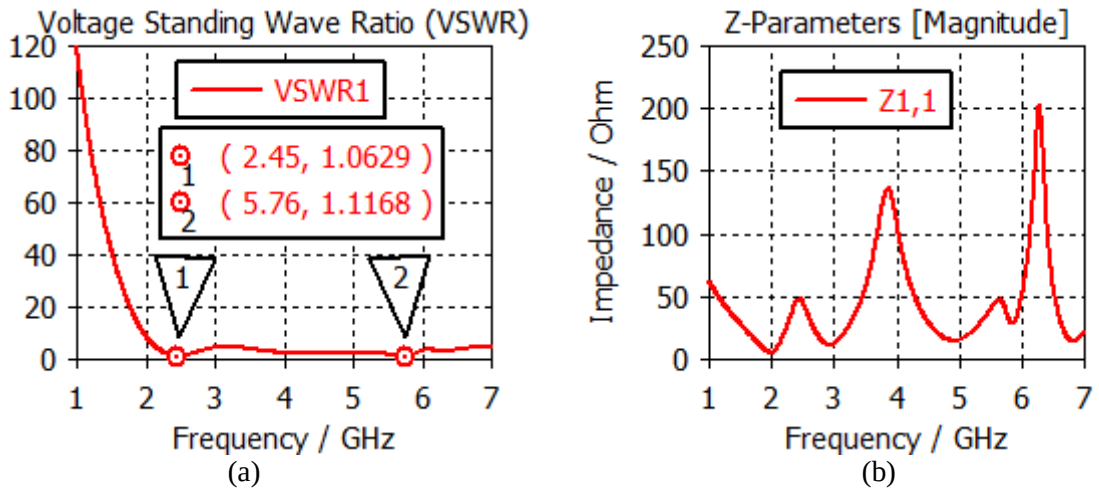

Figure 7. (a) VSWR of proposed antenna and (b) Z- parameters.

4.1 Surface-current Distribution Analysis

To evaluate the performance of the proposed antenna, we conducted simulations of the surface-current distribution at two resonant frequencies, 2.45 GHz and 5.76 GHz (Figure 8). The results exhibit distinct patterns at each frequency, revealing specific operational characteristics of the antenna.

At 2.45 GHz: The surface current predominantly gathers around the feed point, slots and antenna edges. This concentration signifies efficient coupling and radiation at the fundamental resonant frequency. The focus at the feed point ensures effective power transfer from the feed line to the radiating elements, while the distribution along the slots and edges enhances the desired radiation properties.

At 5.76 GHz: The surface current concentrates more around the antenna edges and apertures. This shift corresponds to a higher-order resonant mode, where the shorter wavelength interacts more

prominently with finer structural details of the antenna. The higher frequency alters current propagation, emphasizing areas that enhance radiation efficiency at this frequency.

Antenna Efficiency through Surface-current Distribution: The efficiency of the antenna correlates closely with its surface current distribution. Analysis of current distribution at 2.45 GHz and 5.76 GHz indicates that in both cases, current concentration in specific regions facilitates efficient conversion of input power into radiated electromagnetic waves. The distinct current paths at these frequencies ensure effective operation across the dual-band spectrum.

Moreover, the observed current patterns suggest well-matched impedance at the feed point for both frequencies. This characteristic is critical for minimizing reflections and maximizing power transfer, thereby enhancing the overall antenna efficiency.

In summary, the simulated surface-current distribution underscores the antenna's capability to operate efficiently across its dual-band frequencies. At 2.45 GHz, concentration around the feed point and slots facilitates effective radiation, while at 5.76 GHz, focus near the edges and apertures supports higher frequency performance. These visions confirm the antenna's design effectiveness in achieving dual-band operation with high efficiency.

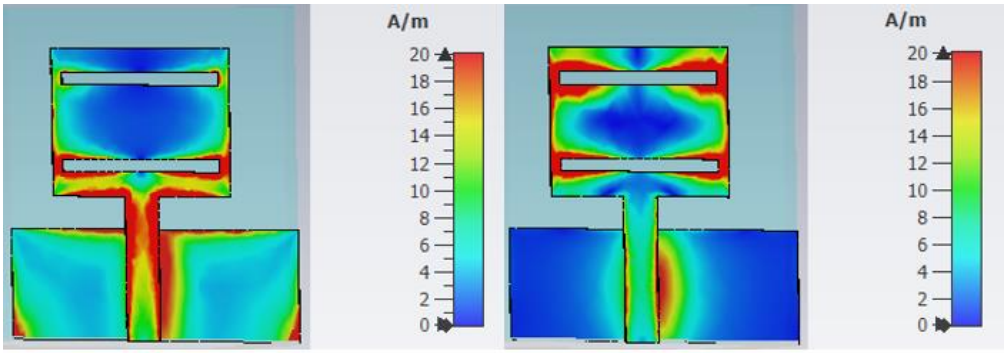

Figure 8. The surface-current distribution of the designed antenna at (a) 2.45 GHz and (b) 5.76 GHz.

4.2 Gain and Efficiency

Figure 9 presents the measured and simulated gain and efficiency of the antenna. At the 2.45 GHz frequency band, the gain is 2.65 dB, while at the 5.76 GHz resonance band, it is approximately 2.8 4 dB. The radiation efficiency at 2.45 GHz is about 95%, demonstrating the antenna's effectiveness in converting input power into radiated energy with minimal losses. This high efficiency is attributed to the optimized design and the incorporation of a Defected Microstrip Structure (DMS), which enhances impedance matching and reduces unwanted radiation and dielectric losses. At 5.76 GHz, the radiation efficiency is around 73%. This efficiency is satisfactory for high-frequency operation, where losses in dielectric and conductive materials are greater than at lower frequencies. Nonetheless, the antenna maintains a commendable level of efficiency across both operating bands. Figure 10 shows the 3D gain and 3D directional radiation pattern.

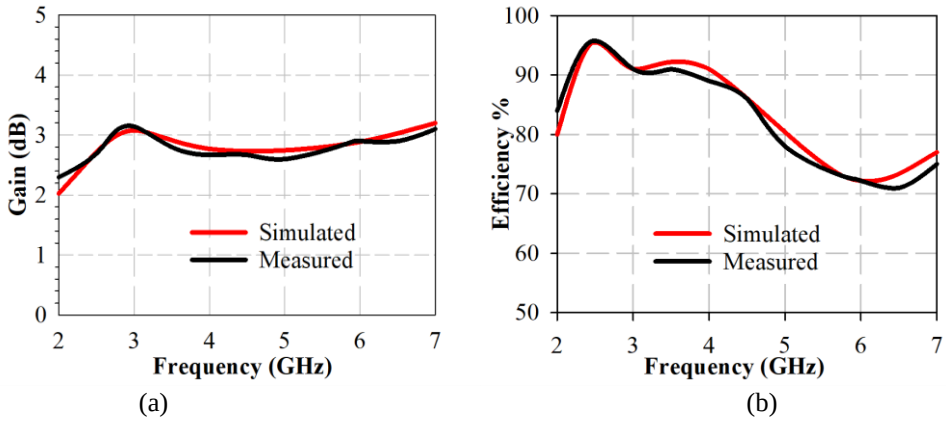

Figure 9. Measured and simulated (a) Peak gain, (b) Radiation efficiency.

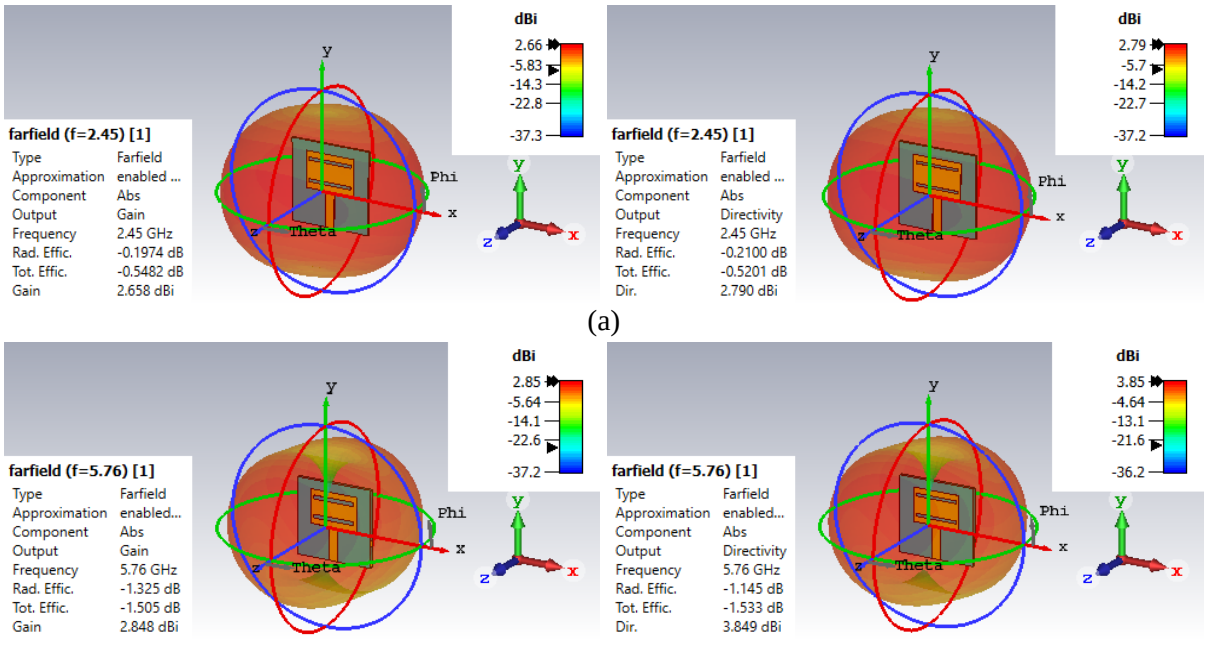

Figure 10. Gain and directivity 3D at (a) 2.45 GHz and (b) 5.76 GHz.

4.3 Radiation Pattern

The measured and simulated radiation patterns of the designed antenna in the E-plane and H-plane are shown in Figure 11. At the lower band (2.45 GHz), depicted in Figure 11(a), the radiation pattern in the E-plane is nearly omnidirectional, while in the H-plane, it is nearly bidirectional. At the upper band (5.76 GHz), shown in Figure 11(b), the antenna exhibits a nearly omnidirectional pattern in the E-plane and a directional pattern in the H-plane. Figure 12 illustrates the Geozondas antenna measurement system that was used to assess the antenna's radiation pattern. A horn antenna was used as the transmitting antenna, while the antenna under examination served as the receiving antenna.

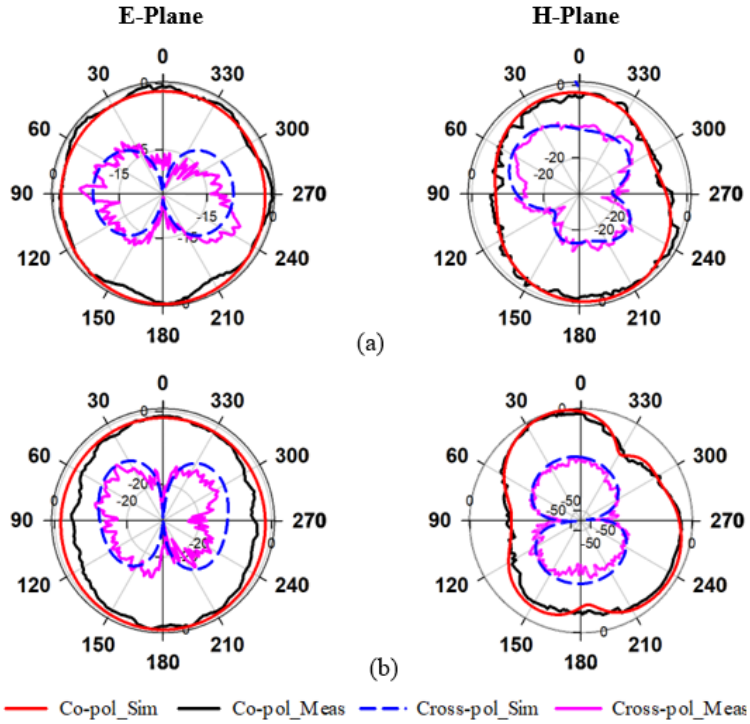

Figure 11. Radiation pattern of the designed antenna in the E-plane and H-plane at (a) 2.45 GHz and (b) 5.76 GHz.

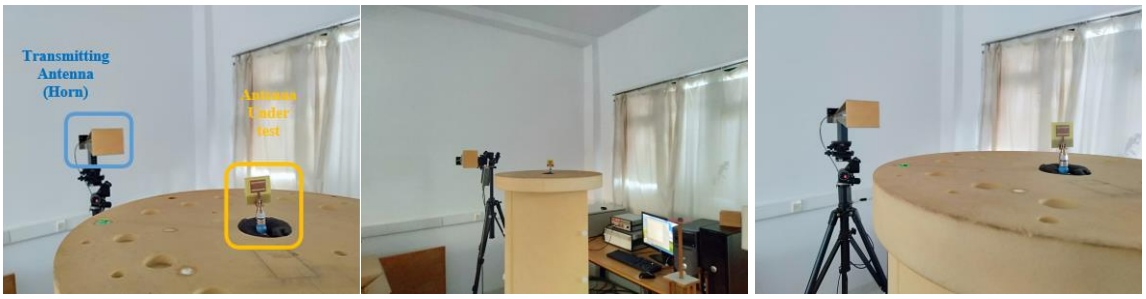

Figure 12. Measurement setup of the designed antenna.

5. PERFORMANCE COMPARISON

A performance comparison has been carried out between the designed antenna and recently reported antennas in the literature in terms of resonant frequencies, size, bandwidth, gain and efficiency, as shown in Table 2. It is observable that the designed antenna has a compact size compared to all the antennas proposed in the references listed in Table 2. In addition, the suggested antenna is distinguished by its elevated efficiency.

Table 2. Comparison of the antenna in this study with antennas proposed in previous studies.

Ref.	Frequency f1/f2 (GHz)	Dimensions (mm^3) Substrate Material	Bandwidth (GHz)	Peaks Gain (dB)	Efficiency (%)
2	2.4/5.2	40 × 30 × 0.8 FR-4	(2.27–2.58)12.7% (4.92–5.49)10.95%	… 	89 87
12	2.54/5.24	40×40×1.524 RogersTMM4	(2.24–2.93)26.69% (4.48–5.54)21.16%	2.5 2.7	…
18	2.4/5.8	47.3 × 55×1.6 FR-4	(2.3–2.492) 7.4% (5.586–6.06) 8.17%	2.5 2.8	…
21	2.4/5.25	52 × 60× 1.6 FR-4	4.2% and 2.3%	2 4.6	…
22	2.45/3.53	59.5×47× 1.6 FR-4	(2.43–2.49)2.44% (3.50–3.56)1.7%	2.45 3.53	…
23	2.45/5.8	70 ×70× 31 3D printed PLA	(2.39–2.52)5.29% (5.76–5.95)3.25%	7.8 6.8	90 80
24	2.44/5.5	52 ×40× 2 FR-4	(2.33–2.86)20.6% (5.76–5.95)15.7%	3.5 3.53	---
This work	2.45/5.76	27 × 27×1.6 FR-4	(2.13–2.88)29.94% (5.65–6.01)6.2%	2.65 2.84	95 73

6. CONCLUSION

This research presents an innovative dual-band patch antenna design with compact dimensions, tailored to meet the requirements of various modern wireless communication systems, including WLAN, ISM, Bluetooth, WiMAX and WiFi-2.4. The antenna operates efficiently at frequencies of 2.45 GHz and 5.76 GHz, achieving high efficiencies of over 95% and 73%, in both operating bands. Additionally, the antenna attains a gain of 2.65 dB at 2.45 GHz and 2.84 dB at 5.76 GHz. The antenna was manufactured and measured, the results being in good agreement with simulations. The measured -10 dB S11 bandwidths cover 750 MHz (2.13-2.88 GHz) and 330 MHz (5.65-6.01 GHz). This ensures that the antenna meets the frequency requirements for WLAN in both the lower and upper bands, ISM (2.4–2.5 GHz), WiMAX rel 1 (2.3–2.4 GHz), WiMAX rel 1.5 (2.5–2.69 GHz) and Bluetooth (2.407–

2.484 GHz). Based on these results and the antenna's characteristics, such as compact size and ease of manufacture, this design is suitable and highly practical for advancing antenna technology and enhancing wireless-communication systems.

REFERENCES

[1] L. C. Paul et al., "Wideband Inset Fed Slotted Patch Microstrip Antenna for ISM Band Applications," Proc. of the 2019 Joint 8th Int. Conf. on Informatics, Electronics & Vision (ICIEV) and 2019 3rd Int. Conf. on Imaging, Vision & Pattern Recognition (icIVPR), pp. 79–84, DOI: 10.1109/ICIEV.2019.8858553, May 2019.

[2] P. B. Nayak, R. Endluri, S. Verma and P. Kumar, "A Novel Compact Dual-band Antenna Design for WLAN Applications," arXiv, DOI: 10.48550/arXiv.2106.13232, May 12, 2021.

[3] P. B. Nayak, S. Verma and P. Kumar, "A Novel Compact Tri-band Antenna Design for WiMAX, WLAN and Bluetooth Applications," Proc. of the 2014 20th National Conf. on Communications (NCC), pp. 1–6, DOI: 10.1109/NCC.2014.6811379, Feb. 2014.

[4] P. B. Nayak, R. Endluri, S. Verma and P. Kumar, "Compact Dual-band Antenna for WLAN Applications," Proc. of the 2013 IEEE 24th Annual Int. Symposium on Personal, Indoor and Mobile Radio Communications (PIMRC), pp. 1381–1385, DOI: 10.1109/PIMRC.2013.6666356, Sep. 2013.

[5] P. Nayak, M. Garetto and E. W. Knightly, "Modeling Multi-user WLANs under Closed-loop Traffic," IEEE/ACM Transactions on Networking, vol. 27, no. 2, pp. 763–776, Apr. 2019.

[6] A. Ghaffar, X. J. Li and B.-C. Seet, "Compact Dual-band Broadband Microstrip Antenna at 2.4 GHz and 5.2 GHz for WLAN Applications," Proc. of the 2018 IEEE Asia-Pacific Conf. on Antennas and Propagation (APCAP), pp. 198–199, DOI: 10.1109/APCAP.2018.8538297, Aug. 2018.

[7] X.-Q. Zhu, Y.-X. Guo and W. Wu, "A Novel Dual-band Antenna for Wireless Communication Applications," IEEE Antennas and Wireless Propagation Letters, vol. 15, pp. 516–519, DOI: 10.1109/LAWP.2015.2456039, 2016.

[8] S. Abulgasem et al., "Antenna Designs for CubeSats: A Review," IEEE Access, vol. 9, pp. 45289–45324, DOI: 10.1109/ACCESS.2021.3066632, 2021.

[9] M. Dube, Design and Fabrication of a Miniaturised Dual Band Planar Antenna for Wireless Communication, PhD Thesis, University of Johannesburg, 2023. [Online], Available: https://ujcontent.uj.ac.za/esploro/outputs/graduate/Design-and-fabrication-of-a-miniaturised/9934308707691, Accessed: Jun. 30, 2024.

[10] M. M. Alam, R. Azim, N. M. Sobahi, A. I. Khan and M. T. Islam, "A Dual-band CPW-fed Miniature Planar Antenna for S-, C-, WiMAX, WLAN, UWB and X-band Applications," Scientific Reports, vol. 12, no. 1, Article no. 1, DOI: 10.1038/s41598-022-11679-7, May 2022.

[11] J. Ali, S. Abdulkareem, A. Hammoodi, A. Salim, M. Yassen and H. Al-Rizzo, "Cantor Fractal-based Printed Slot Antenna for Dual-band Wireless Applications," Int. Journal of Microwave and Wireless Technologies, vol. 8, no. 2, pp. 263–270, DOI: 10.1017/S1759078714001469, Mar. 2016.

[12] M. T. Yassen, M. R. Hussan, H. A. Hammas, H. Al-Saedi and J. K. Ali, "A Dual-band Printed Antenna Design Based on Annular Koch Snowflake Slot Structure," Wireless Pers. Commun., vol. 104, pp. 649–662, DOI: 10.1007/s11277-018-6039-0, 2019.

[13] G. Rushingabigwi, L. Sun, Q. Zhu, Y. Xia and Y. Yu, "Design and Realization of a Dual Wide Band Printed Monopole Antenna for WiFi and WiMAX Systems," IJCNS, vol. 09, no. 05, pp. 184–197, DOI: 10.4236/ijcns.2016.95018, 2016.

[14] R. Roshan, S. Prajapati, H. Tiwari and G. Govind, "A Dual Wideband Monopole Antenna for GSM/UMTS/LTE/WiFi/and Lower UWB Application," Proc. of the 2018 3rd Int. Conf. on Microwave and Photonics (ICMAP), pp. 1–2, DOI: 10.1109/ICMAP.2018.8354635, Feb. 2018.

[15] B. P. Nadh, B. T. P. Madhav and M. S. Kumar, "Design and Analysis of Dual Band Implantable DGS Antenna for Medical Applications," Sādhanā, vol. 44, no. 6, p. 131, DOI: 10.1007/s12046-019-1099-8, May 2019.

[16] H. Yao, X. Liu, H. Zhu, H. Li, G. Dong and K. Bi, "Dual-band Microstrip Antenna Based on Polarization Conversion Metasurface Structure," Frontiers in Physics, vol. 8, 2020. [Online], Available: https://www.frontiersin.org/articles/10.3389/fphy.2020.00279, Accessed: Oct. 30, 2023.

[17] L. C. Paul, H. K. Saha, T. Rani, R. Azim, M. T. Islam and M. Samsuzzaman, "A Dual-band Semi-circular Patch Antenna for WiMAX and WiFi-5/6 Applications," Int. Journal of Communication Systems, vol. 36, no. 1, p. e5357, DOI: 10.1002/dac.5357, 2023.

[18] R. H. Thaher and Z. S. Jamil, "Design of Dual Band Microstrip Antenna for Wi-Fi and WiMax Applications," TELKOMNIKA (Telecommunication Computing Electronics and Control), vol. 16, no. 6, Article no. 6, DOI: 10.12928/telkomnika. v16i6.10016, Dec. 2018.

[19] A. A. Yassin, R. A. Saeed and R. A. Mokhtar, "Dual-band Microstrip Patch Antenna Design Using C-slot for WiFi and WiMax Applications," Proc. of the 2014 Int. Conf. on Computer and Communication Engineering, pp. 228–231, DOI: 10.1109/ICCCE.2014.72, Sep. 2014.

[20] C.A. Balanis, Antenna Theory Analysis and Design, 2nd Edn, J. Wiley & Sons, New York, 2016.

[21] S. Luo, Y. Li, Y. Xia, G. Yang, L. Sun and L. Zhao, "Mutual Coupling Reduction of a Dual-band Antenna Array Using Dual-frequency Metamaterial Structure," The Applied Computational Electromagnetics Society Journal (ACES), vol. 2019, pp. 403–410, Mar. 2019.

[22] I. Zahraoui et al., "A New Planar Multiband Antenna for GPS, ISM and WiMAX Applications," Int. Journal of Electrical and Computer Engineering (IJECE), vol. 7, no. 4, Article no. 4, DOI: 10.11591/ijece. v7i4. Pp 2018-2026, Aug. 2017.

[23] K. N. Olan-Nuñez and R. S. Murphy-Arteaga, "Dual-band Antenna on 3D-Printed Substrate for 2.4/5.8 GHz ISM-band Applications," Electronics, vol. 12, no. 11, p. 2368, 2023.

[24] X. Wu, X. Wen, J. Yang, S. Yang and J. Xu, "Metamaterial Structure Based Dual-band Antenna for WLAN," IEEE Photonics Journal, vol. 14, no. 2, pp. 1-5, 2022.

ملخص البحث:

تقدم هذه الوقة البحثية هوائياً ذا نطاقين ترددّيين مصمّماً لأنظمة الاتّصالات اللاسلكية. ويعمل الهوائي المقترح بفاعلية عند تردّد 2.45 جيجاهيرتز وتردّد 5.76 جيجاهيرتز، محقّقاً أداءً عالياً على الرّغم من صغر حجمه. وقدّ تمّ استخدام بنية الشّريط الميكروي المنحرف (DMS) للحصول على النّطاقين التّردّديّين المرغوبين وتحسين توافق الممانعات عند التّردّدات المطلوبة. وتمّ تجميع الهوائي المقترح على طبقة أساس من نوع FR-4 بأبعاد بلغت (27 ملم × 27 ملم × 1.6 ملم). وقد بلغت فعالية المحاكاة عند التّردّدين 2.45 جيجاهيرتز و 5.76 جيجاهيرتز 95% و 73% على الترتيب. أما كسْب الهوائي المقترح فبلغ أكبر من 2.65 ديسيبل وحوالي 2.84 ديسيبل عند النّطاقين التّردّديين المرغوبين على الترتيب.

والجدير بالذّكر أنّ الهوائي المقترح تمّت محاكاتُه وتصنيعه وفحْصه والتّحقُّق من خصائصه عملياً. أمّا فقْد الإرجاع المقاس عند الرّنين الأدنى والرّنين الأعلى فكان 29.94% مغطياً النّطاق التّردّدي من 2.13 جيجاهيرتز إلى 2.88 جيجاهيرتز، و 6.2% مغطّياً النّطاق التردّدي من 5.65 جيجاهيرتز إلى 6.01 جيجاهيرتز على التّرتيب. كذلك تمّت المقارنة بيْن نمط الإشعاع المقاس للهوائي المقترح ونمط الإشعاع للهوائي المقترح عن طريق المحاكاة، حيث اتّفقا بشكلٍ كبير.

ويتميز الهوائي المقترح ببساطة تصميمه وسهولة تصنيعه وصغر حجمه، مع عمله بشكلٍ جيّد عند التّردّدات الّتي صُمّم لها، الأمر الّذي يجعله ملائماً للاستخدام في أنظمة الاتّصالات اللاسلكية.